

Close-up of mushroom-shaped fibrillar adhesive microstructure: contact element behaviour

M Varenberg and S Gorb

J. R. Soc. Interface 2008 **5**, 785-789
doi: 10.1098/rsif.2007.1201

References

This article cites 18 articles, 8 of which can be accessed free

<http://rsif.royalsocietypublishing.org/content/5/24/785.full.html#ref-list-1>

Email alerting service

Receive free email alerts when new articles cite this article - sign up in the box at the top right-hand corner of the article or click [here](#)

To subscribe to *J. R. Soc. Interface* go to: <http://rsif.royalsocietypublishing.org/subscriptions>

Close-up of mushroom-shaped fibrillar adhesive microstructure: contact element behaviour

M. Varenberg* and S. Gorb

Department of Thin Films and Biological Systems, Max Planck Institute for Metals Research, Heisenbergstrasse 3, Stuttgart 70569, Germany

To analyse the performance of mushroom-shaped fibrillar adhesive microstructure, its behaviour was studied during different stages of attachment–loading–detachment cycle. Visualizing the evolutions of real contact area of single microfibres, it is shown that the mushroom-shaped geometry of contact elements promotes fast and simple generation of reliable adhesion. The mushroom-shaped geometry seems to transform fibrillar contact elements into passive suction devices and makes them tolerant to overload, thus enhancing their robustness and stability. These findings may also be extrapolated to biological fibrillar attachment devices sharing the same geometry.

Keywords: biomimetics; surface patterning; polymer; adhesion

1. INTRODUCTION

Biological fibrillar attachment systems have received much research attention for years, and works of Autumn *et al.* (2000), Gorb *et al.* (2001) and Niederegger & Gorb (2006) are just a few recent examples illustrating the efforts made to understand the ability of some reptiles, insects and arachnids to adhere to a wide variety of surfaces. Two general types of terminal contact elements are identified in these systems: spatula-shaped and mushroom-shaped elements. The spatula-shaped contact elements require active lateral loading for proper functioning (Niederegger & Gorb 2003; Tian *et al.* 2006) and are associated with a muscle-driven temporary attachment involved in locomotion (Stork 1980; Autumn *et al.* 2006). The mushroom-shaped contact elements are passive attachment devices able to hold for a virtually unlimited period of time with no muscular mechanism being invoked, which are used in a long-term process of pairing (Stork 1980). The dynamics of the contact behaviour of these systems remains, however, poorly studied. There were a few attempts to visualize the behaviour of terminal contact elements found in flies and beetles (Niederegger *et al.* 2002; Hosoda & Gorb submitted), but, in general, the operating principles of biological fibrillar attachment systems are judged from purely morphological data.

Based on the analysis of the tarsal hairs found in numerous species of beetles from the family Chrysomelidae, an effective biomimetic mushroom-shaped fibrillar adhesive microstructure has recently been produced (Daltorio *et al.* 2005; Varenberg & Gorb 2007; Gorb *et al.* 2007). This microstructure offers a unique way to

model the contact behaviour of biological mushroom-shaped fibrillar contact elements in varying conditions, which would otherwise be extremely difficult. Visualizing the dynamic process of contact separation may also shed more light on the effect of contact element geometry on dry adhesion (Sitti & Fearing 2003; Peressadko & Gorb 2004; Crosby *et al.* 2005; Spolenak *et al.* 2005; Kim & Sitti 2006; Gorb *et al.* 2007; Gorb & Varenberg 2008).

In light of the above, the purpose of the present work was to study the dynamics of the contact behaviour of mushroom-shaped fibrillar adhesive microstructure. This was accomplished by analysing the evolutions of real contact area of single microfibres during different stages of attachment–loading–detachment cycle.

2. EXPERIMENTAL DETAILS

The study was performed with an optical stereomicroscope Leica MZ 12.5 (Leica GmbH, Wetzlar, Germany) equipped with a coaxial light source and a monochrome high-speed digital camera Kodak Motion Corder Analyzer SR-Ultra (Eastman Kodak Co., San Diego, CA). Specimens tested were structured polyvinylsiloxane (PVS) discs of 2 mm in diameter and 1 mm in height mounted on a three-axis motorized micromanipulator DC3314R (World Precision Instruments, Inc., Sarasota, FL), which was driven at a velocity of approximately 1 mm s^{-1} to load the specimens against a fixed 5 mm thick glass substrate (figure 1). Structured surface (Gottlieb Binder GmbH, Holzgerlingen, Germany) consisted of hexagonally distributed mushroom-shaped microfibres of approximately 100 μm in height bearing terminal contact plates of 48 μm in mean diameter (figure 2). Destructive interference of

*Author for correspondence (varenberg@mf.mpg.de).

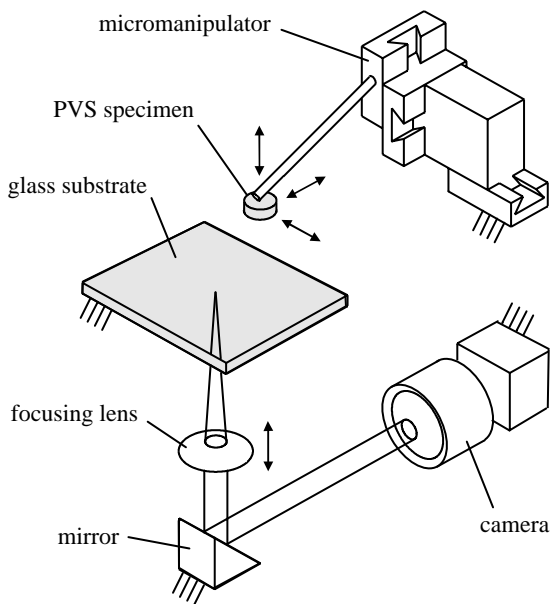


Figure 1. Schematic of the experimental set-up.

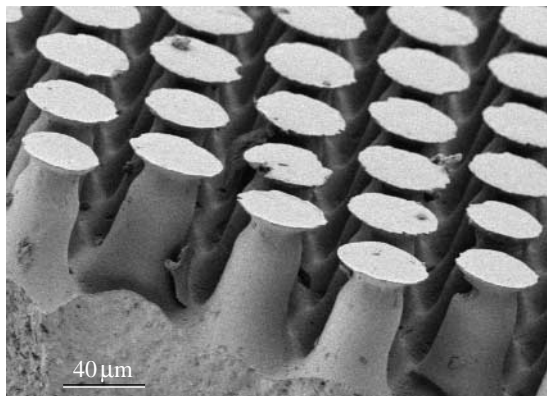


Figure 2. Mushroom-shaped microfibres forming contact surface of structured PVS specimens.

reflected white light in the glass–PVS interface resulted in a visualization of the real contact area and allowed the analysis of its evolutions during different loading stages. The load applied was controlled manually based on the appearance of the contact area and was not determined quantitatively.

To get an insight into how mushroom-shaped microfibres deform when in contact, the microstructure was fixed between two cover glasses joined by screws and imaged in a Hitachi S-4800 high-resolution scanning electron microscope at an accelerating voltage of 3 kV. The load applied by the screws was adjusted based on the contact appearance changes visible by optical microscopy and was not determined quantitatively.

3. RESULTS AND DISCUSSION

3.1. Routine function

3.1.1. Contact formation. Figure 3 shows the behaviour of mushroom-shaped fibrillar adhesive microstructure coming in contact with the substrate. The series of still

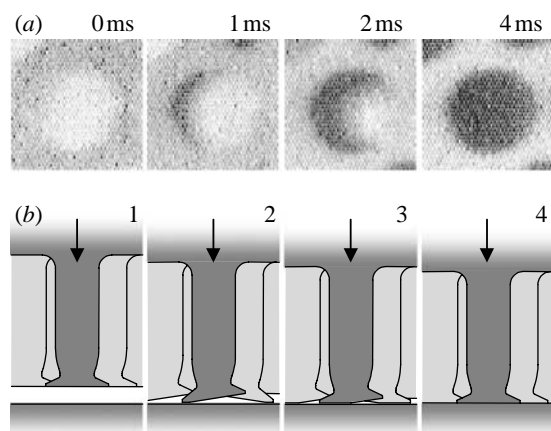


Figure 3. Attachment of mushroom-shaped fibrillar microstructure. (a) Behaviour of a single terminal contact plate attaching to the substrate. Dark areas represent the real contact zones. (b) Schematic of a mushroom-shaped micro-fibre attaching to the substrate. Drawn in accordance with still images in (a); arrow in the direction of specimen motion.

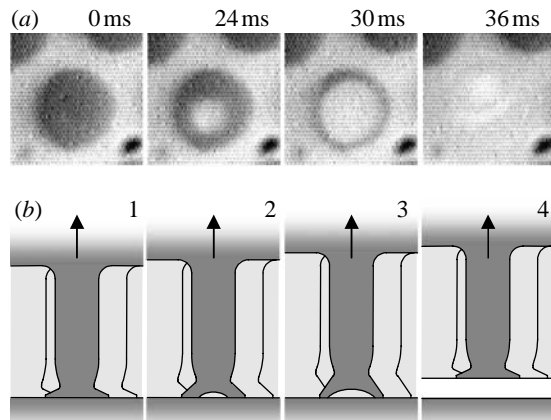


Figure 4. Detachment of mushroom-shaped fibrillar microstructure. (a) Behaviour of a single terminal contact plate detaching from the substrate. Dark areas represent the real contact zones. (b) Schematic of a mushroom-shaped micro-fibre detaching from the substrate. Drawn in accordance with still images in (a); arrow in the direction of specimen motion.

images depicting changes in contact area (figure 3a) clearly indicates that single microfibres jump in contact within few milliseconds, which correlates well with the driving velocity. In all likelihood, terminal contact plates are never ideally oriented in parallel to the substrate. Hence, the attachment of each contact plate initiates at the edge that is closest to the mating surface. Then, the contact zone formed grows towards the opposite edge until the entire contact plate is attached. The thin contact plate lip is much easier to deform than the central part of the contact plate (figure 3a). This promotes faster attachment, as the longer is the line of the contact front propagation progresses along the circumference of the contact plate (figure 3a). This promotes faster attachment, as the longer is the line of the contact front propagation, the larger is the contact area increment per unit time. Analysing the process of contact formation presented in figure 3a, one can anticipate that the attachment of

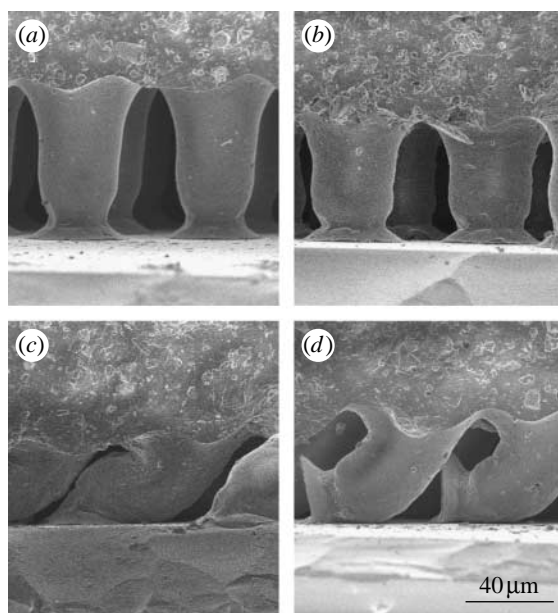


Figure 5. Mushroom-shaped microfibres in (a) an unloaded state, (b) under pure compression, (c) under pure compression distorted by slight shear and (d) under large shear.

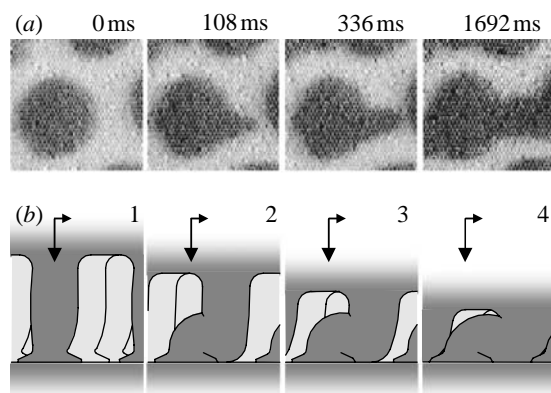


Figure 6. Compression of mushroom-shaped fibrillar microstructure. (a) Behaviour of a single terminal contact plate in distorted compression. Dark areas represent the real contact zones. (b) Schematic of a mushroom-shaped microfibre collapsing due to a distorted compression. Drawn in accordance with still images in (a); arrows in the direction of the load.

mushroom-shaped fibrillar adhesive microstructure develops according to the schematic diagram depicted in figure 3b.

3.1.2. Contact rupture. Once the full contact is formed, it is no longer possible to activate a peeling mode of separation when a mushroom-shaped contact element is detached from the substrate (Gorb & Varenberg 2008). As each mushroom-shaped microfibre is pulled off, a void is formed in the centre and grows towards the edge of the contact plate until it is finally detached from the substrate (figure 4a). Thus, despite being flat (figure 2), each contact plate acts as a passive suction device when the thin elastic contact plate lip does not allow the surrounding air to enter the low-pressure void

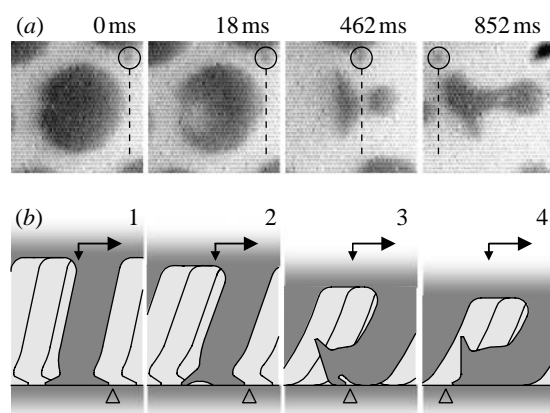


Figure 7. Shearing of mushroom-shaped fibrillar microstructure. (a) Behaviour of a single terminal contact plate in large shear. Dark areas represent the real contact zones. Open circle highlights a point marker located on the substrate surface. Horizontal distance between the marker and the right edge of the contact plate changes on the last image, thus denoting sliding inception. (b) Schematic of a mushroom-shaped microfibre bending due to a large shear. Drawn in accordance with still images in (a); open triangle points to the hypothetical position of the marker; arrows in the direction of the load.

formed due to the microfibre stalk tension (figure 4b). Interestingly, this finding seems to contradict previous observations on attachment ability of beetles bearing mushroom-shaped setae (Stork 1980), which discredited a suction hypothesis by exhibiting no reduction in adhesion under reduced pressure of the surrounding atmosphere. However, this contradiction can be neutralized if the presence of a liquid secretion on beetles' adhesive setae is taken into account. In liquid, which is nearly inextensible, the decrease in pressure balances the expansive force until the pressure falls to the cavitation threshold (Smith 1991) and liquid is turned into vapour under the terminal contact plate to allow its deformation required for detachment (Varenberg & Gorb 2008; figure 4b). Cavitation pressure is constant for a given temperature, and therefore the suction device bearing a liquid layer should not lose its attachment ability when the pressure of the surrounding atmosphere is reduced. Thus, our finding suggests that similar to the *Dytiscus* cup-shaped adhesive structures analysed in the early eighteenth century (Derham 1713), mushroom-shaped setae in males of Chrysomelidae beetles, which use a liquid secretion in attachment system, act as passive suction devices.

3.2. Overloading

To understand whether mushroom-shaped fibrillar microstructure is stable enough under field conditions when the load cannot be precisely controlled, it was also necessary to study its tolerance to overloading. It was found that the microstructure can withstand large elastic deformations without losing adhesive contact with the substrate when under pure compression (figure 5a,b). Superposition of a shearing load resulted, however, in a more complicated behaviour of the

microfibres (figure 5c,d) and, depending on whether the shearing was dominant, the deformation of the microfibres resulted in different contact performances.

3.2.1. Shear-distorted compression. Figure 6 presents the behaviour of mushroom-shaped fibrillar microstructure in compression. The series of still images in figure 6a clearly demonstrates that terminal contact plates are able to stay attached even under extremely high loads when the microfibres collapse due to a slight shear and tend to rupture the contact. This tolerance, however, seems to be a function of the microfibre spacing. If they are dense enough, at some load, the collapsed microfibre stalks start to press the adjacent terminal contact plates to the substrate, thus preventing them from detachment (figures 6b and 5c). This behaviour makes the system tolerant to compression, and facilitates its adhesive function by allowing for overloading during contact formation and enhancing its robustness and stability.

3.2.2. Large shearing. Observing the contact area changes induced by shearing (figure 7a), one can see that the microfibres are not able to resist large tangential load and the contact plates terminating the structured surface gradually lose their contact with the substrate. Similar to a simple contact rupture described in §3.1.2, a low-pressure void is formed under the contact plate (figure 7b2). However, due to the asymmetry of the shearing load, it grows in one direction and eventually reaches the contact edge, releasing an internal pressure deficit and switching the contact from suction to peeling mode of separation. Partial detachment of the contact plate leads to a larger bending of the microfibre stalk, which finally comes in contact with the substrate (figure 7b3). Additional shearing results in an overturn of the contact plate (figures 7b4 and 5d), and causes sliding inception. This stage is visualized by changes in a relative position between the right edge of the contact plate and the point marker located on the substrate surface (figure 7a). The first three images share the same position of a single microfibre, which is attached to the left of the marker. The fourth image demonstrates the same microfibre situated to the right of the marker, thus pointing to sliding inception. Interestingly, the microstructure is unable to generate any pull-off force at this stage and can be easily separated from the substrate (Varenberg & Gorb 2007). Hence, it may be suggested that animals bearing mushroom-shaped fibrillar adhesive elements use shearing motion to release themselves from contact. Nevertheless, the microstructure is tolerant to shearing until the peeling mode of separation is dominant and can routinely function within certain limits of the tangential load applied (Varenberg & Gorb 2007).

4. CONCLUSION

The study performed shows that the mushroom-shaped geometry of fibrillar contact elements is

responsible for a stable adhesive attachment. This type of contact element promotes fast and simple generation of reliable adhesion. The mushroom-shaped geometry seems to transform fibrillar contact elements into passive suction devices and makes them tolerant to overload, thus enhancing their robustness and stability. Considering that the microstructure tested is a biomimetic model system, the above findings shed insight into the behaviour of biological attachment devices sharing the same geometry.

This work was supported by the Federal Ministry of Education, Science and Technology, Germany (project InspiRat 01RI0633C).

REFERENCES

Autumn, K., Liang, Y. A., Hsieh, S. T., Zesch, W., Chan, W. P., Kenny, T. W., Fearing, R. & Full, R. J. 2000 Adhesive force of a single gecko foot-hair. *Nature* **405**, 681–685. ([doi:10.1038/35015073](https://doi.org/10.1038/35015073))

Autumn, K., Dittmore, A., Santos, D., Spenko, M. & Cutkosky, M. 2006 Frictional adhesion: a new angle on gecko attachment. *J. Exp. Biol.* **209**, 3569–3579. ([doi:10.1242/jeb.02486](https://doi.org/10.1242/jeb.02486))

Crosby, A. J., Hageman, M. & Duncan, A. 2005 Controlling polymer adhesion with “pancakes”. *Langmuir* **21**, 11 738–11 743. ([doi:10.1021/la051721k](https://doi.org/10.1021/la051721k))

Daltonio, K. A., Gorb, S., Peressadko, A., Horchler, A. D., Ritzmann, R. E. & Quinn, R. D. 2005 A robot that climbs walls using micro-structured polymer feet. In *Proc. Int. Conf. Climbing and Walking Robots, London, UK*, pp. 131–138.

Derham, W. 1713 *Physico-theology: or, a demonstration of the being and attributes of God, from his works of creation*. London, UK: W. Innys.

Gorb, S. N. & Varenberg, M. 2008 Mushroom-shaped geometry of contact elements in biological adhesive systems. *J. Adhes. Sci. Technol.* **21**, 12–13. ([doi:10.1163/156856107782328317](https://doi.org/10.1163/156856107782328317))

Gorb, S., Gorb, E. & Kastner, V. G. 2001 Scale effects on the attachment pads and friction forces in syrphid flies (Diptera, Syrphidae). *J. Exp. Biol.* **204**, 1421–1431.

Gorb, S., Varenberg, M., Peressadko, A. & Tuma, J. 2007 Biomimetic mushroom-shaped fibrillar adhesive microstructure. *J. R. Soc. Interface* **4**, 271–275. ([doi:10.1098/rsif.2006.0164](https://doi.org/10.1098/rsif.2006.0164))

Hosoda, N. & Gorb, S. Submitted. Limits of the attachment ability of insect hairy pads: a case study on the beetle *Gastrophysa viridula*.

Kim, S. & Sitti, M. 2006 Biologically inspired polymer microfibers with spatulate tips as repeatable fibrillar adhesives. *Appl. Phys. Lett.* **89**, 261 911. ([doi:10.1063/1.2424442](https://doi.org/10.1063/1.2424442))

Niederegger, S. & Gorb, S. 2003 Tarsal movements in flies during leg attachment and detachment on a smooth substrate. *J. Insect Physiol.* **49**, 611–620. ([doi:10.1016/S0022-1910\(03\)00048-9](https://doi.org/10.1016/S0022-1910(03)00048-9))

Niederegger, S. & Gorb, S. 2006 Friction and adhesion in the tarsal and metatarsal scopulae of spiders. *J. Comp. Physiol. A* **192**, 1223–1232. ([doi:10.1007/s00359-006-0157-y](https://doi.org/10.1007/s00359-006-0157-y))

Niederegger, S., Gorb, S. & Jiao, Y. 2002 Contact behavior of tenent setae in attachment pads of the blowfly *Calliphora vicina* (Diptera, Calliphoridae). *J. Comp. Physiol. A* **187**, 961–970. ([doi:10.1007/s00359-001-0265-7](https://doi.org/10.1007/s00359-001-0265-7))

Peressadko, A. & Gorb, S. N. 2004 When less is more: experimental evidence for tenacity enhancement by division of contact area. *J. Adhes.* **80**, 247–261. ([doi:10.1080/00218460490430199](https://doi.org/10.1080/00218460490430199))

Sitti, M. & Fearing, R. S. 2003 Synthetic gecko foot-hair micro/nano-structures as dry adhesives. *J. Adhes. Sci. Technol.* **17**, 1055–1074. ([doi:10.1163/156856103322113788](https://doi.org/10.1163/156856103322113788))

Smith, A. M. 1991 Negative pressure generated by octopus suckers: a study of the tensile strength of water in nature. *J. Exp. Biol.* **157**, 257–271.

Spolenak, R., Gorb, S., Gao, H. & Arzt, E. 2005 Effects of contact shape on the scaling of biological attachments. *Proc. R. Soc. A* **461**, 305–319. ([doi:10.1098/rspa.2004.1326](https://doi.org/10.1098/rspa.2004.1326))

Stork, N. E. 1980 A scanning electron microscope study of tarsal adhesive setae in the Coleoptera. *Zool. J. Linn. Soc.* **68**, 173–306.

Tian, Y., Pesika, N., Zeng, H., Rosenberg, K., Zhao, B., McGuigan, P., Autumn, K. & Israelachvili, J. 2006 Adhesion and friction in gecko toe attachment and detachment. *Proc. Natl. Acad. Sci. USA* **103**, 19 320–19 325. ([doi:10.1073/pnas.0608841103](https://doi.org/10.1073/pnas.0608841103))

Varenberg, M. & Gorb, S. 2007 Shearing of fibrillar adhesive microstructure: friction and shear-related changes in pull-off force. *J. R. Soc. Interface* **4**, 721–725. ([doi:10.1098/rsif.2007.0222](https://doi.org/10.1098/rsif.2007.0222))

Varenberg, M. & Gorb, S. 2008 A beetle-inspired solution for underwater adhesion. *J. R. Soc. Interface* **5**, 383–385. ([doi:10.1098/rsif.2007.1171](https://doi.org/10.1098/rsif.2007.1171))